GAVIN PUBLISHERS

Journal of Ophthalmology Research & Reports

De Keizer RJW, et al. Ophthalmol Res Rep 4: 130.

Research Article

Two-Photon Microscopy to Visualize Amyloid-Beta Plaques in Retinas from Alzheimer's Disease

Francisco J Ávila[1], Laura Emptage[2], Melanie CW Campbell[2,3], Juan M Bueno[1*]

[1]Laboratorio de Óptica, Instituto Universitario de Investigación en Óptica y Nanofísica, Universidad de Murcia, Campus de Espinardo, Murcia, Spain

[2]Physics & Astronomy, University of Waterloo, Waterloo, Canada

[3]School of Optometry and Vision Science, University of Waterloo, Waterloo, Canada

***Corresponding author:** Juan M Bueno, Laboratorio de Óptica, Instituto Universitario de Investigación en Óptica y Nanofísica, Universidad de Murcia, Campus de Espinardo (Edificio 34), 30100 Murcia, Spain, Tel: +34 868 88 8335; E-mail: bueno@um.es

Citation: Bueno JM, Avila JF, Emptage L, Campbell CWM (2019) Two-photon microscopy to visualize amyloid-beta plaques in retinas from Alzheimer's disease. Ophthalmol Res Rep 4: 130.

Received Date: 10 January, 2019; **Accepted Date:** 16 January, 2019; **Published Date:** 24 January, 2019

Abstract

Alzheimer's Disease (AD) is a neurodegenerative pathology which progresses with age and is the most common cause of dementia. AD is characterized by the formation of Amyloid-β (Aβ) plaques that are insoluble in the extracellular matrix of the brain, causing dystrophy of adjacent cells. The analysis of the spatial distribution and morphology of Aβ deposits can help to characterize AD progression and to develop techniques for early diagnosis of the disease. We explored here two-photon microscopy as a new tool to visualize amyloid deposits in fixed retinal tissues of human donors, and a dog used as a natural animal model. Deposits provided higher signal than the adjacent tissues and were located lying on the retinal nerve fiber layer and penetrating slightly into it. These results suggest that two-photon microscopy can be used as a non-invasive technique to visualize amyloid plaques in non-stained retinal tissues, which might help in AD diagnosis.

Keywords: lzheimer; Amyloid;MultiphotonMicroscopy; Retina

Introduction

Alzheimer's Disease(AD) is a progressive neurodegenerative disorder, characterized by the accumulation of perphosphorylatedτ-protein in neurofibrillary tangles and insoluble fibrils (plaques or deposits) composed of Amyloid-β (Aβ) protein in the extracellular space of the brain [1]. In the brain, senile Aβ deposits are mainly distributed along the cortex and also present in the hippocampus. Over the past 30 years, the typical criteria of AD diagnosis have included probable factors as dementia, mild cognitive impairment and preclinical symptoms [2]. More recently, the advances in neuropsychology have allowed identifying prodromal AD in patients with cognitive impairment [3]. However the only definitive way to diagnose AD is to locate plaques and tangles in brain tissue, which is determined by means of biopsy or autopsy after death [4].

Since no definitive diagnosis prior to death is currently available, the development of imaging methods to visualize Aβplaques is a field of interest to facilitate AD detection. In particular, some neuroimaging techniques have been reported to be sensitive to amyloid location in the brain; including Positron Emission Tomography (PET), Photon Emission Computed Tomography (SPECT) and Magnetic Resonance

Imaging (MRI). PET presents low resolution (~6 mm) with respect to the average diameter of Aβ plaques in the brain (0.06mm) [5,6] and thus it not able to spatially resolve individual plaques. SPECT achieves resolutions less than a 1mm but the sensitivity is even lower than PET [7,8]. MRI provides higher spatial resolution (between 0.1 and 1mm) but with also low sensitivity [9,10]. Moreover, ppolarization properties of stained Aβ have been studied in brain tissue. In combination with Congo red, Aβis brief ringent as seen under crossed polarizer's[11] and can used as a biomarker [12]. Two-Photon Excitation Fluorescence (TPEF) techniques allow high-resolution imaging (~1 μm) of microscopic structures and optical tomography with a restricted excitation volume (i.e. out-of-plane photobleaching is avoided) [13,14]. In TPEF microscopy, infrared light provides fluorescence which otherwise require levels of ultraviolet radiation with high risk of photodamage. This long-wavelength light leads to deeper tissue penetration and tissues markers are not required.

In particular, senile Aβ plaques have been imaged with TPEF microscopy in the brain of in vivo AD animal models [15]. The detected fluorescence was carried out by injecting a contrast agent (Thioflavine-S) into the brain. Different experiments have demonstrated the presence of Aβ deposits in (ex vivo and in vivo) brain tissue of both humans and animal models [16-18]. TPEF and second harmonic signal have also been analyzed in unstained brain slices of ttransgenic mice [19]. Although it is well known that Aβ deposits are present in neural tissue when AD is established [20], the use of TPEF microscopy to obtain in vivo imaging of the brain as a diagnosis method of AD, is unfortunately very invasive.

On the other hand, Aβ deposits have also been found in the neural layers of postmortem retinal tissues from human donors affected by AD [21] and in retinas of animal models [22,23], using atomic force microscopy and fluorescence labeling techniques, respectively. Results were consistent with brain pathology and clinical reports. Moreover, ours are the first measurements of the polarization properties of Aβ deposits in retinal tissue [24,25], including their visibility in crossed polarization.

The neural retina is optically accessible, so any technique able to detect Aβ deposits in the eye will be of great interest to understand and track AD. Since all retinal layers has been reported to provide TPEF signal [26], the aim of this work is to propose TPEF microscopy as an alternative non-invasive method to visualize Aβ deposits in unstained retinal tissues. Retinas from both AD-affected human donors and a beagle dog suffering from cognitive impairment were analyzed. The inherent co focal properties of TPEF microscopy will allow the optical sectioning of the samples, and therefore the assessment of the longitudinal size (along depth) of Aβ deposits within the retina.

Methods

Experimental system: TPEF microscope

A mode-locked Ti:Sapphire laser used as illumination source (λ=760 nm, pulses of 120 as at 76 MHz) was coupled into an inverted commercial microscope [26]. The light reached the sample through a non-immersion microscope objective (20x, NA=0.5). The non-linear signal from the sample was detected in the backward direction via the same microscope objective. This passed through a spectral filter (TPEF filter, 435-700 nm) and reached the photomultiplier tube. A Diachronic Mirror (DM) was used to separate the excitation from the emission wavelengths. Images were recorded in the XY plane using a scan unit composed of a pair of non-resonant galvanometric mirrors. A Z-scan motor coupled to the microscope objective allowed optical sectioning. It was used to locate the focal plane along the Z axis and to acquire stacks of images for different depth positions, in order to get 3D volume renderings.

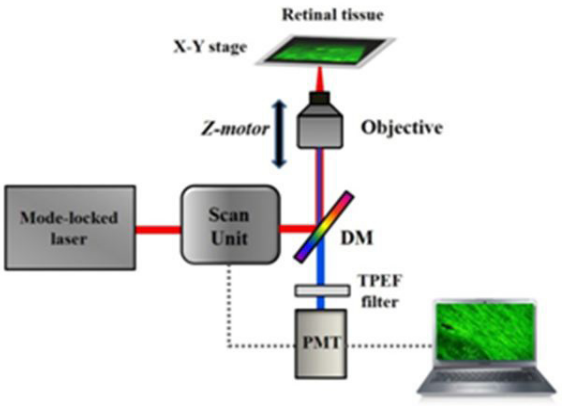

Figure 1: Schematic diagram of the multiphoton microscope (see text for details).

Samples

Four partial retinas from both four human donors (samples #1-#4) with a diagnosis of AD (and age matched normal without AD or glaucoma) and a beagle dog suffering from

a naturally occurring cognitive dysfunction syndrome were analyzed. The latter is an animal model for retinal pathology in AD, since its Aβ amino acid sequence is identical to that of human beings. Moreover, symptoms and brain pathology of this dysfunction syndrome are similar to similar to those produce by AD.

Human retinas were dissected from eyes obtained following informed consent under the auspices of the Eye Bank of Ontario. The dog was categorized by a battery of non-verbal cognitive function test. The animal was euthanized for unrelated reasons and one of the retinas was analyzed. The retinas were fixed in par formaldehyde solution overnight, flap-mounted on a microscope slide and covered with a cover slip. One of the samples (#1) was stained with 0.1 % Thioflavine-S. This was used as a test to ensure that the deposits imaged with TPEF microscopy corresponded to Aβ deposits [27].

Experimental TPEF imaging

In previous experiment, the specimens were firstly placed between crossed polarizer's with the microscope operating in bright-field mode. This allowed a faster location of the areas with presumed Aβ deposits [24,25] used for the posterior TPEF imaging. Then, at different retinal locations containing deposits, series of TPEF images (210x210 μm2) were acquired at different depth positions throughout the retina (from the inner retinal structures to the photoreceptors outer segments). Further details on TPEF imaging can be found elsewhere [26]. Image processing was performed with MatLab TM custom-written software. 3D images were reconstructed using the public domain image processing software ImageJ and the Aβ deposit isolation method was performed with the UCSF Chimera package.

Results

TPEF Imaging of Human Retinas

Figure 2 shows TPEF images of different human retinal areas containing deposits with different morphology, density and distribution. In particular, (Figure 2a) corresponds to sample #1, the retina stained with Thioflavine-S. The deposit was positive to staining and showed polarization contrast, what confirm that the imaged deposit was Aβ type [27]. In a large deposit, such as this one, it can also be observed how the edges show stronger TPEF signal which permits a better visualization of the plaque morphology.

This is probably a side effect of the labeling procedure, not present in the rest of samples. In all cases, a visual inspection reveals that Aβ deposits provide stronger TPEF signal than surrounding retinal structures. Moreover Aβ deposits were mainly located over the nerve fibers layer, although in some cases they slightly penetrate into it. It is worth noticing that the measured signal corresponds to endogenous fluorescence (i.e. the sample's autofluorescence) arising from specific molecules.

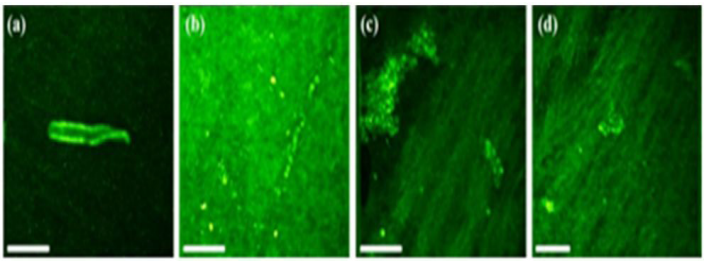

Figure 2: TPEF images containing Aβ deposits in different human retinal tissues (samples #1-#4). Bar length: 50 μm.

Figure 3 shows a set of six TPEF images of sample in (Figure 2a) (sample #1) acquired at different depth locations starting at the first inner retinal layer providing TPEF signal (i.e. the Aβdeposit, Figure 3a). When imaging deeper into the sample, the retinal nerve fiber layer and some ganglion cells are visible (Figure 3c and 3d). Once the Aβ deposit is above the section, a shadowed area with lower TPEF signal and surrounded brighter structures can be seen.

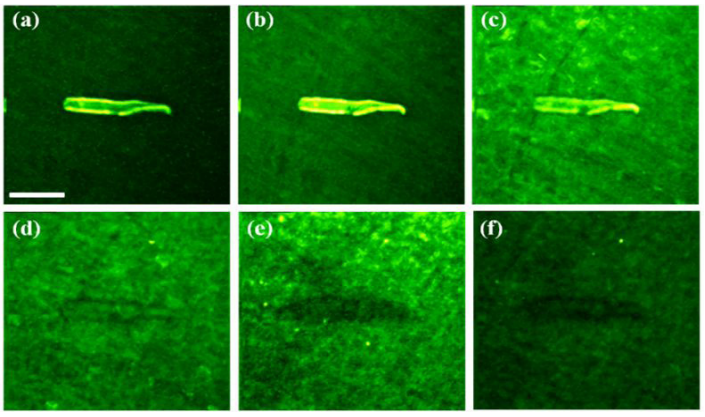

Figure 3:Set of TPEF images of an Aβdeposit at different retinal depth locations. The specimen is the same as that in Figure 2a.

Another example of Aβdeposits and retinal structures in a human sample (#2) is presented (Figure 4). The deposit and some retinal structures are easily visualized in (Figure 4a-c). Beneath the Aβ deposit (located close to the ganglion

cell layer in this sample), the corresponding shadow lying over the photoreceptor mosaic is observed (Figure 4f).

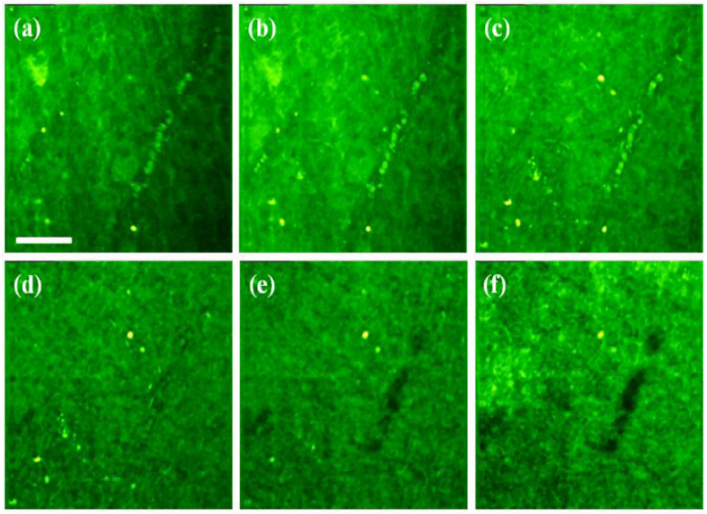

Figure 4: Set of TPEF images containing an Aβ deposit as a function of retinal depth. The sample is the same as in Figure 2b.

For the sense of completeness, (Figure 5) presents an additional set of TPEF images as a function of depth (around the retinal nerve fiber layer) for the sample in (Figure 2d) (for the sample in (Figure 2c), results were similar). In this example, the deposits were found near the top of the nerve fiber layer (Figure 5a,b), again having higher TPEF intensity levels that the adjacent structures. However when increasing the section depth, it can easily be observed how these deposits penetrate into the nerve fiber layer (Figure 5c,d). When going deeper (Figure 5e,f), it disappears and the fibers appear intact (i.e. with absence of Aβ)

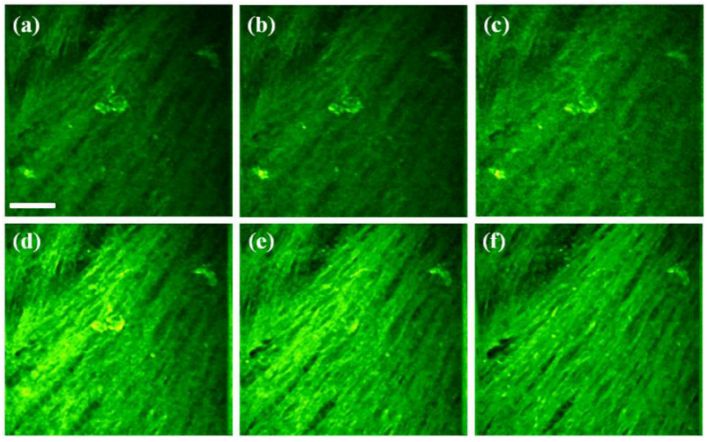

Figure 5: TPEF images from sample in Figure 2d recorded at different depths. Bar scale: 50 μm.

From the stacks of TPEF images along the Z direction, optical sectioning and 3D renderings of the retina can be done. These provide detailed and valuable information of the dimensions and morphology of the Aβ deposits. For samples #1 and #3, (Figure 6) depicts the corresponding volume renderings (from 15 images each) where 3D views of the deposits are shown. It is evident that the maximum fluorescence signal comes from the deposits. Moreover, the estimated thickness of these Aβ deposits was respectively 32 and 20 μm.

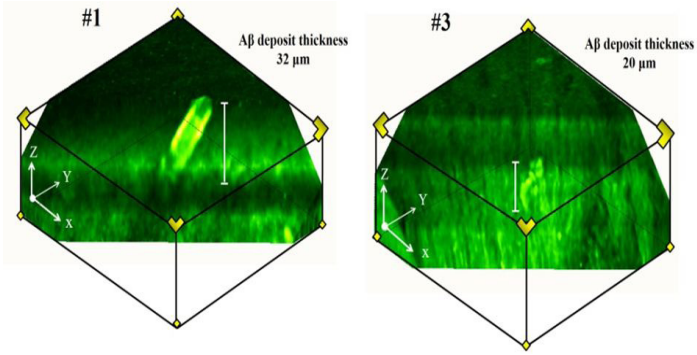

Figure 6: Reconstructed volume renderings of samples #1 and #3. The reconstruction was carried out using stacks of 15 images spaced 5 and 2 μm, respectively. The estimated thickness of the Aβ deposit is indicated with a white bar.

TPEF Imaging in Dog Retinas

This section presents the results on Aβ deposit TPEF imaging in an animal model of Alzheimer's disease with cognitive impairment (sample #5). (Figure 7) shows TPEF images from two different locations containing Aβ deposits in a dog retina. Similar to the human specimens, the retinal areas with deposits were imaged at different depth locations. Illustrative examples are depicted in (Figure 8,9). In (Figure 8f and 9f) the photoreceptor layer is clearly displayed. Finally, the reconstructed volume renderings are shown in (Figure10). The estimated Aβ thickness values for the locations were 27 and 21 μm, respectively.

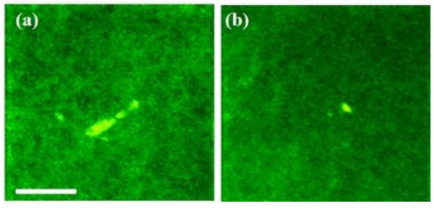

Figure 7: TPEF images of two locations containing Aβ deposits in a dog retinal tissue. Bar length: 50 μm.

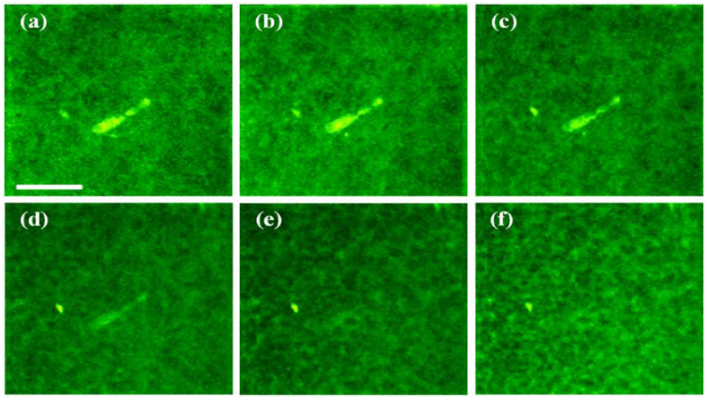

Figure 8: TPEF images containing an Aβ deposit as a function of retinal depth. The sample is that in Figure 8a. Bar length: 50 μm.

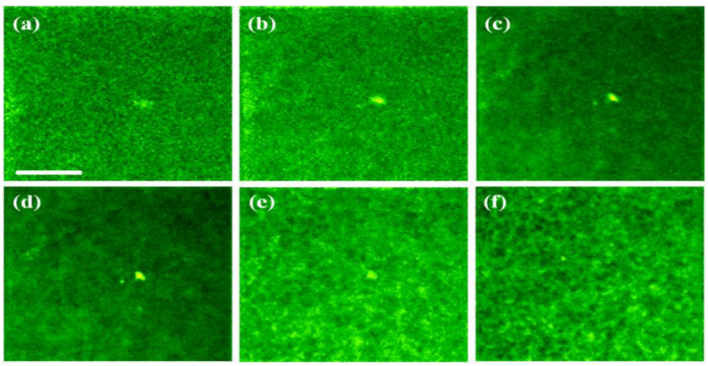

Figure 9: TPEF images of a dog retina acquired at different depths locations (the retinal area is that shown in Figure 8b). Bar scale: 50 μm.

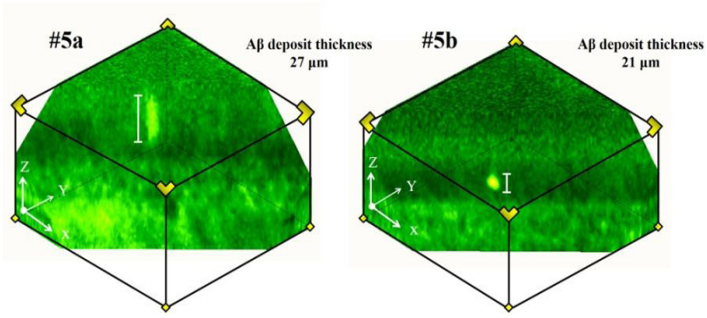

Figure 10: 3D reconstructed images of the two retinal locations of Figure 7.

TPEF Imaging of Isolated AβDeposits

Once volume renderings are reconstructed from the stacks of TPEF images (see for instance Figure 6 and 10), UCSF software was used to isolate the Aβ deposit from retinal tissue. (Figure 12) shows 3D visualizations of isolated Aβ deposits corresponding to samples #1 and #2 (human tissue) and #5 (dog retina). The thickness of the deposits computed from these images was 32 and 27 μm for samples #1 and #5 respectively. The thickness value for the deposits shown in sample #2 ranged between 15 and 40 μm in depth.

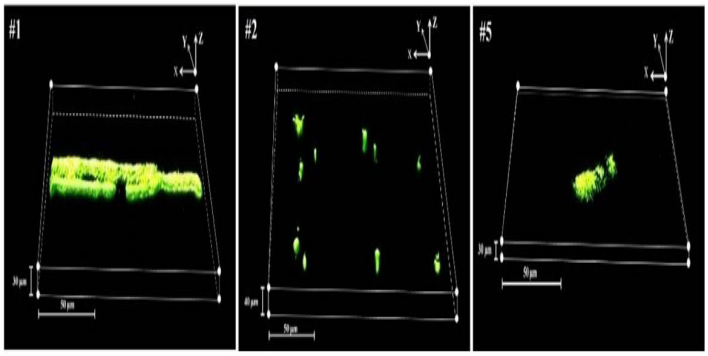

Figure 11: Reconstructed 3D Aβ deposits isolated from the surrounding retinal structure

Discussion and Conclusions

In the present work, a TPEF microscope has successfully been used to visualize Aβ deposits in retinas of human donors with a diagnosis of AD and a beagle dog suffering from cognitive impairment. The instrument represents a useful non-invasive imaging tool, offering high resolution imaging without noticeable photodamage. The optical sectioning capabilities of TPEF techniques also allowed 3D reconstruction of the imaged structures. These might help to better visualize the areas of interest and to provide additional information about the size, location, spatial organization and morphology of Aβ plaques.

Although TPEF microscopy has been used to explore different retinal structures [28-35], to our knowledge, this is the first time that it has been used to image Aβ plaques in retinal tissues. Results herein confirm that retinal Aβ plaques exhibit auto fluorescencein both humans and dogs. This agrees with previous multiphoton experiments carried out in the brain of transgenic AD mice [19]. Moreover, it has been shown that Aβ deposits provide higher TPEF signal levels than the normal retinal structures. This enhances the visualization, which facilitates their location across the different retinal areas. This also allows visualizing both the plaques and retinal cells without labeling procedures.

TPEF images have demonstrated that for both, human and dog retinas, the Aβ deposits are mainly located at the inner retina. In particular, they are lying in front of nerve

fiber layer and slightly penetrating into it. This corroborates that the beagle dog is a useful and valuable animal model to explore analyze AD in retinal tissues. The morphology and location of the deposits depend on both the sample and the retinal location. This variability was also reported in brain plaques of AD mouse models [19]. The stacks of individual frames acquired along the Z-direction have allowed the reconstruction of volume renderings of the areas of interest. These representations provide detailed information of the retinal morphology. Moreover, the 3D TPEF images corresponding to isolated Aβ plaques allow obtaining more detailed information of the shape and size. It has been reported that the optic nerve of patients diagnosed of AD showed degeneration of retinal ganglion cells and their axons in the fiber layer [36] as well as abnormalities in retinal vascular parameters [37]. There is also evidence that visual disturbances in patients with AD are caused by pathological changes in the optic nerve [38]. All these damages could also be related to the presence of Aβdeposits. Since the progression of AD is related to an increase in Aβ deposits in neural tissue, the analysis of the spatial distribution of Aβ could help to better understand and potentially track AD as well as the effects of therapies.

To conclude, TPEF microscopy has successfully been used to image presumed Aβplaques in fixed retinas of AD-affected human donors and a beagle dog suffering from cognitive impairment. Results demonstrated that the TPEF signal from plaques is different and higher than that from surrounding retinal tissue, what facilitates the characterization of their morphology and size. Nevertheless the results here presented must be understood as a preliminary study on the use of TPEF signals for the detection of Aβ plaques in AD retinas. Additional experiments are required to corroborate the performance and accuracy of the technique. These might include the characterization of Aβ spectral fluorescence and the use of fresh retinas from donors suffering from with AD at different stages, among others.

Acknowledgments

This work has been supported by the Canadian Institutes of Health Research, Natural Sciences and Engineering Research Council of Canada and the Spanish SEIDI (grant FIS2013-41237-R).

References

1. BraakH, BraakE (1991) Neuropathologicalstageing of Alzheimer-related changes,ActaNeuropathol 82: 239-259.
2. McKhann G, Drachman D, FolsteinM, Katzm an R, Price Dn , et al. (1984) Clinical diagnosis of Alzheimer´s disease, Neurology 34: 939.
3. Sarazin M, Berr C, Berr C (2007) Amnestic syndrome of the medial temporal type identifies prodromal AD: a longitudinal study, Neurology 69: 1859-1867.
4. Gearing M,Mirra SS, Hedreen JC, Sumi SM, Hansen L A, et al. (1995) The Consortium to Establish a Registry for Alzheimer 's disease(CERAD)-part X. neuropathology confirmation of the clinical diagnosis of Alzheimer's disease, Neurology 45: 461-466.
5. Bacskai BJ, Klunk WE, Mathis CA, Hyman BT (2002) Imaging Amyloid-β Deposits In VivoJ Cerebral Blood flow & Metabolism 22:1035-1041.
6. Noble M, Scarmeas N (2009) Application of pet imaging to diagnosis of Alzheimer's disease and mild cognitive impairment. Int RevNeurobiol 84:133-149.
7. WeberDA, Ivanovic M,Franceschi D, Strand S.E, Erlandsson K, et al. (1994)Pinhole SPECT: an approach to in vivo high resolution SPECT imaging in small laboratory animals.JNucl Med35:342-348.
8. Ono M (2009) Development of positron-emission tomography/single-photon emission computed tomography imaging probes for in vivo detection of beta-amyloid plaques in Alzheimer's brains. Chem Pharm Bull 57:1029-1039.
9. Cavagna FM, Dapra M, Castelli PM, Maggioni F, Kirchin MA (1997). Trends and developments in MRI contrast agent research, EurRadiol7:222-224.
10. Benveniste H, Ma Y,Dhawan J, Gifford A, Smith SD, et al. (2007) Anatomical and functional phenotyping of mice models of Alzheimer's disease by MR microscopy. Ann Y AcadSci 1097:12-29.
11. DivryP, Florkin CR (1927)Sur les propriétées optiques de l'amyloide.C R SocBiol 97 :1808-1810.
12. Puchtler H, Waldrop FS, Meloan SN (1985) A review of light, polarization and fluorescence microscopic methods for amyloid.ApplPathol 3: 5-17.

13. Denk W, Strickler JH, Webb WW (1990) Two-photon laser scanning fluorescence microscopy. Science 248 :73-76.

14. Williams RM, Zipfel WR, Webb WW (2001) Multiphoton microscopy in biological research, CurrOpinChemBiol5: 603-608.

15. Christie RH, Bacskai BJ, Zipfel WR, Williams RM, Kajdasz ST, et al. (2001)GrowthArrest of IndividualSenile Plaques in a Model of Alzheimer'sDiseaseObserved by In Vivo MultiphotonMicroscopy. J Neuroscience21: 858-864.

16. McLellan ME, Kajdasz ST, Hyman BT, Bacskai BJ (2003) In Vivo Imaging of ReactiveOxygenSpeciesSpecifically-AssociatedwithThioflavine S-Positive Amyloid Plaques by MultiphotonMicroscopy. J Neuroscience 23 :2212-2217.

17. Meyer-Luehmann M, Spires-Jones TL, Prada C, Garcia-Alloza M, Calignon A, et al. (2008) Rapidappearance and local toxicity of amyloid-β plaques in a mouse model of Alzheimer'sdisease, Nature 451 :720-724.

18. Jung CK, Keppler K, Steinbach S, Blazquez-Llorca L, Herms J (2015) FibrillarAmyloid Plaque Formation PrecedesMicroglial Activation. PLoS ONE 10 : e0119768.

19. Kwang A C,Duff K, Gouras GK, Webb WW (2008) Optical visualization of Alzheimer´spathology via multiphoton-excitedintrinsic fluorescence and second harmonic-generation. OptExpress 17:3679-3688.

20. Cohen R M, Rezai-Zadeh K, Weitz T M, Rentsendorj A, Gate D, et al. (2013)A transgenic Alzheimer rat with plaques, tau pathology, behavioral impairment,oligomericAβ and frank neuronal loss. J Neurosci 33: 6245-6256.

21. Campbell MCW, Gowing L, Choi Y, Leonenko Z (2010) Imaging of amyloid-beta deposits in the post-mortem retina in Alzheimer's disease. InvestOphthalmol ViSci 51 : 5778.

22. Koronyo-Hamaoui M, Koronyo Y, Ljubimov AV, Miller CA, Ko MK, et al. (2011) Identification of amyloid plaques in retinas fromAlzheimer'spatients and noninvasive in vivo opticalimaging of retinal plaques in a mouse model.Neuroimage54 : S204-S217.

23. Emptage L, DeVries D, Kisilak M, Campbell M C, Leonenko Z, et al. (2015) Comparison of amyloid beta in the retina of an animal model of Alzheimer's disease and humans with the disease,ARVO Meeting Abstracts 56:4250.

24. Avila FJ, Emptage L, Kisilak ML, Bueno JM, Campbell M C W (2013)Polarimetry in ex vivo retina from donors with Alzheimer's disease, ARVO Meeting Abstracts 54: 2304.

25. DeVries D, Campbell M C W, Emptage L, Cookson C, Kisilak M, et al. (2015), Polarization properties of amyloid β deposits differ from surrounding ex vivo human retinas from those with Alzheimer's disease, ARVO Meeting Abstracts 56:2385.

26. Bueno JM, Giakoumaki A, Gualda E J, Schaeffel F,Artal P (2011)Analysis of the chicken retina with an adaptive optics multiphoton microscope, Biomed Opt Express 2:1637-1148.

27. Campbell MC, DeVries D, Emptage L, Cookson C, Zisilak M, et al. (2015) "Polarizationproperties of amyloid beta in the retina of theeye as a biomarker of Alzheimer'sdisease". Optics in theLifeSciences OSA TechnicalDigestBM3A: 4.

28. Imanishi Y, Batten M L, Piston D W, Baehr W, Palczewski K, (2004)Noninvasive two-photon imaging reveals retinyl ester storage structures in the eye. J Cell Biol 164:373-383.

29. Han M, Bindewald-Wittich A, Holz FG, Giese G, Niemz M H, et al. (2006)Two-photon excited autofluorescence imaging of human retinal pigment epithelial cells. J Biomed Opt 11:010501.

30. Gualda EJ, Bueno JM, Artal P (2010) Wave front optimized non-linear microscopy of ex-vivo human retinas J Biom Opt 15:026007.

31. Bueno JM, Gualda E J, Artal P (2010)Adaptive optics multiphoton microscopy to study ex vivo ocular tissues. J Biom Opt 15:066004.

32. Lu R-W, Y Li C, Ye T,Strang C,Keyser K, et al. (2011) Two-photon excited autofluorescence imaging of freshly isolated frog retinas, Biomed. Opt. Express 2:1494-1503.

33. Hunter JJ, Masella B, Dubra A, Sharma R, Yin L, et al. (2011) "Images of photoreceptors in living primate eyesusingadaptiveopticstwo-photonophthalmoscopy". BiomedOpt Express 2:139-148.

34. Bueno JM,Palacios R, Giakoumaki A, Gualda EJ, Schaeffel F, et al. (2014). Retinal cell imaging in myopic chickens using adaptive optics multiphoton microscopy, Biomed. Opt. Express 5: 664-674.

35. He S, Ye C, Sun Q, Leung KS C, Qu J Y (2015)Label-free nonlinear optical imaging of mouse retina,Biomed Opt Express 6:1055-1066.

36. Sadun AA, Basi CJ (1990)Optic nerve damage in Alzheimer's disease.Ophthalmology 97:917.

37. Frost S, Kanagasingam Y, Sohrabi H, Vignarajan J, Bourgeat P, et al. (2013)Retinal vascular biomarkers for early detection and monitoring of Alzheimer's disease, Trans Psychiatry 3: e233.

38. Berisha, Feke GT, Trempe CL, McMeel JW, Schepens CL (2007) "Retinal Abnormalities in Early Alzheimer's Disease." InvestOphthal VisSci 48: 2285-2289.